

RESEARCH PAPER

MECHANICAL DAMPING CHARACTERISTICS OF DUCTILE AND GREY IRONS MICRO-ALLOYED WITH COMBINATIONS OF Mo, Ni, Cu AND Cr

Sylvester Olanrewaju Omole^{1*}, Kenneth Kanayo Alaneme^{1,2}, Akinlabi Oyetunji¹¹Department of Metallurgical and Materials Engineering, School of Engineering and Engineering Technology, Federal University of Technology, Akure, PMB 704. Ondo State Nigeria.²Centre for Nano Engineering and Tribo Corrosion, School of Mining, Metallurgical and Chemical Engineering, University of Johannesburg, Johannesburg South Africa.*Corresponding author: sylvesteromole@yahoo.com, soomole@futa.edu.ng Tel. 2347033089934, Department of Metallurgical and Materials Engineering, Federal University of Technology, Akure. P. M. B 704. Ondo State Nigeria.

Received: 10.12.2020

Accepted: 24.01.2021

ABSTRACT

Damping behaviour of ductile and grey cast irons micro alloyed with combinations of Mo, Ni, Cu and Cr, was investigated in this study. This was aimed at establishing the effect of composition and microstructural parameters on the damping properties of the micro alloyed cast irons. Grey cast iron was micro alloyed randomly with molybdenum, nickel, chromium and copper at an amount not more than 0.2 % each; magnesium was added to the melt in ladle prior to casting. The microstructures showed that ductile iron was formed and grey iron was also formed due to insufficient 'nodulizer', the ductile iron consisted of pearlite and ferrite phases with their nodular graphite. The micro-alloyed ductile iron generally had higher storage (78906 – 120868 MPa) and loss modulus (5375 – 6715 MPa) than that of the grey cast iron and ductile iron composition without alloying elements. Although the damping capacity of the composition without micro alloying elements was initially higher for all the cast irons (~ 0.085), but failed at approximately 110 °C, while most of the micro-alloyed ductile irons exhibited relatively satisfactory capacity for vibration energy dissipation up to 190 °C than the micro-alloyed grey irons.

Keywords: Damping; microalloying; mechanical, ductile and grey cast iron, temperature; frequency

INTRODUCTION

The utilization of ductile irons has increased globally as a result of its good mechanical properties, low cost of production, and adaptability for mass production [1]. However, they possess moderate to low corrosion, fracture, wear resistance and damping capacity – properties that are now critical requirements for several nascent automobile and machinery components [2, 3]. This has raised concerns about the continued suitability of ductile irons, for the design of these mechanical systems [4]. This development has challenged the iron metallurgy community to explore ways of enhancing the material property spectrum of ductile irons while still maintaining low cost processing which has been an age long attraction for ductile irons [5, 6].

Several researchers have explored the use of micro alloying elements such as nickel, copper, chromium, molybdenum, among others to improve the properties of ductile irons [7]. Rao et al. [8] reported that manganese/copper ratio can be optimally selected for enhanced pearlite formation, which results in improved mechanical properties in ductile irons. Similar outcome was achieved with the use of manganese, nickel, molybdenum, and copper as micro alloying addition, as long as the composition of these elements did not exceed 0.5% [9].

It has been reported that optimal selection of combinations of Mo, Cr, Ni and Cu as micro alloying addition in ductile irons,

results in improved strength, toughness and wear resistance [10, 11]. However, the effect of these micro alloying additions on the damping properties of ductile irons has not come under scrutiny. High damping capacity is considered as one of the required properties needed in the selection of material for several machinery and automobile elements, where high vibration damping resistance is very critical for optimal service performance [12]. The performance of dynamic mechanical and construction equipment, often results in undesirable vibration which have negative impact on the life of the machine [13]. Generally, the damping capacity of cast irons is reported to be influenced by factors such as the internal friction mechanism of the graphite, graphite volume fraction, count and morphology, matrix structure, matrix phase surrounding the graphite, presence of alloying elements, among others [14-16]. These microstructural variables are largely dependent on the composition, and processing deployed for the cast iron production [17, 18]. Pereira et al. [19] stated that generally, any material that has the capacity to dissipate energy of vibration otherwise known as loss modulus, will minimize noise and vibration. In the case of ductile irons, solid solution strengthening of the ferritic matrix phase of a ductile iron as well as increase in the nodule density, was reported to help improve the damping capacity in ductile irons. However, the impact on these phase and graphite parameters and the consequential effect on the damping properties of the specific alloy combinations selected as micro-alloying additions in this

study, to the best of our knowledge has not received attention from literature.

Hence, the aim of this study is to evaluate the influence of the selected microalloying combinations on the mechanical damping properties (storage modulus, loss modulus and damping capacity) of the ductile and grey irons developed. The research questions which the present study intends to provide answers to are: does the micro alloying composition influence damping properties of the ductile irons produced? How are the damping properties influenced by the test conditions such as test frequency and temperature? What are the underlying mechanisms responsible for the damping characteristics displayed by the ductile irons? Are these postulations supported by microstructural evidences? That is, can the microstructures help elucidate the damping behaviour manifested by the ductile irons? It is envisaged that the outcomes from the investigation will help establish the reliability of the selected micro alloying combinations for practical utilization of ductile irons in component design for automobile and machinery applications, where an excellent balance of damping, mechanical and wear properties are desirable.

MATERIAL AND METHODS

Ductile Irons Production

The procedures adopted for the production of the ductile irons have been reported in details by Omole et al. [10, 11]. The process summarily, involved utilization of grey cast iron scrap as base metal, while ferro-molybdenum (72%), ferro-chrome (64% Cr), copper and nickel, were utilized as micro alloying additions. Ferrosilicon magnesium (5 % Mg, 45 % Si), graphite (as recarburiser), calcium carbide (as sulphur removal) and calcium carbonate (as flux), were other materials utilized as casting additives. Seven charge compositions were prepared for the ductile iron production with micro alloying combinations and weight percent, added in proportions as presented in **Table 1**.

The cast irons were produced by melting the base metal (grey iron scraps) and then adding the respective alloying elements to

the melt. The melt was super-heated to 1430 °C and then tapped into a ladle containing magnesium in the ladle pocket and was cast to produce the ductile irons. Cast irons were allowed to solidify to room temperature in green sand mould before knockout of the castings in the mould. The chemical compositions of the cast irons produced are shown in **Table 2**. After the production, it was noted that two of the seven compositions did not develop ductile iron structures but that of grey irons, thus the compositions were designated AG1 and AG2, to distinguish them from the other compositions which developed nodular structures.

Characterization with Optical Microscope

Each specimen was first prepared through metallographic processes of grinding and polishing. This was done using different grits of grinding and polishing paper with pastes to obtain a mirror finished surface. The polished surfaces were etched using 4% nital for 10 seconds. The structures were examined with Zeiss optical microscope with Axiom5 camera attachment.

Damping Test

Assessment of the damping properties of both the ductile and grey irons were carried out on a Dynamic Mechanical Thermal Analyzer (DMTA) using three-point bending mode in accordance with ASTM 756 -05 (2017) [20] standard. Specimens used for this study were machined to a flat rectangular shape of dimension 5 mm width by 2 mm thickness and 55 mm length. The thermal analysis determines the stiffness of the materials under the application of dynamic load as a function of temperature, frequency, amplitude and time. The test was performed using strain amplitude of $2 \mu\text{m}$ (2×10^{-6}), vibration frequency of 1 and 5 Hz, temperature range of room temperature to 200 °C and heating rate of 5 °C per minute. The parameters evaluated are: the storage modulus (dynamic modulus) (E'), loss modulus (E'') and damping capacity (also known as $\tan \delta$) – which was determined using the relation [21]:

$$\tan \delta = \frac{E''}{E'} \quad (1.)$$

Table 1 Charges Combination for Melting in the Furnace

Melt/ Sample	Initial Charge Material in the Furnace
AD1	Fe scrap, graphite (C), Si, Mn (in base metal), 0.15%Mo, 0.15%Ni, 0.15%Cu
AD2	Fe scrap, graphite (C), Si, Mn (in base metal), 0.15%Mo, 0.15%Ni
AD3	Fe scrap, graphite (C), Si, Mn (in base metal), 0.15%Cu, 0.15%Cr
AD4	Fe scrap, graphite (C), Si, Mn (in base metal), 0.15%Mo, 0.15%Ni, 0.15%Cr
D5	Fe scrap, graphite (C), Si, Mn (in base metal),
AG1	Fe scrap, graphite (C), Si, Mn (in base metal), 0.15%Mo, 0.15%Cr, 0.15%Cu
AG2	Fe scrap, graphite (C), Si, Mn (in base metal), 0.15%Ni, 0.15%Cu, 0.15%Cr

Note: AD denotes alloyed ductile iron, D5 unalloyed ductile iron and AG denotes alloyed grey iron

Table 2 Chemical Composition of the Specimens Produced

6.5	AD1	AD2	AD3	AD4	D5	AG1	AG2
CE	4.27	4.38	4.14	4.23	4.18	4.16	4.33
%C	3.42	3.50	3.20	3.40	3.30	3.30	3.45
%Si	2.50	2.60	2.80	2.45	2.62	2.53	2.60
%Mn	0.35	0.39	0.53	0.50	0.42	0.58	0.47
%Mo	0.11	0.19	-	0.24	-	0.13	-
%Ni	0.16	0.22	-	0.18	-	-	0.16
%Cr	-	-	0.12	0.10	-	0.11	0.11
%Cu	0.20	-	0.21	-	-	0.19	0.19
%Mg	0.073	0.086	0.095	0.091	0.081	0.039	0.032
%S	0.030	0.034	0.026	0.031	0.027	0.026	0.030
%P	0.048	0.042	0.030	0.048	0.029	0.041	0.042

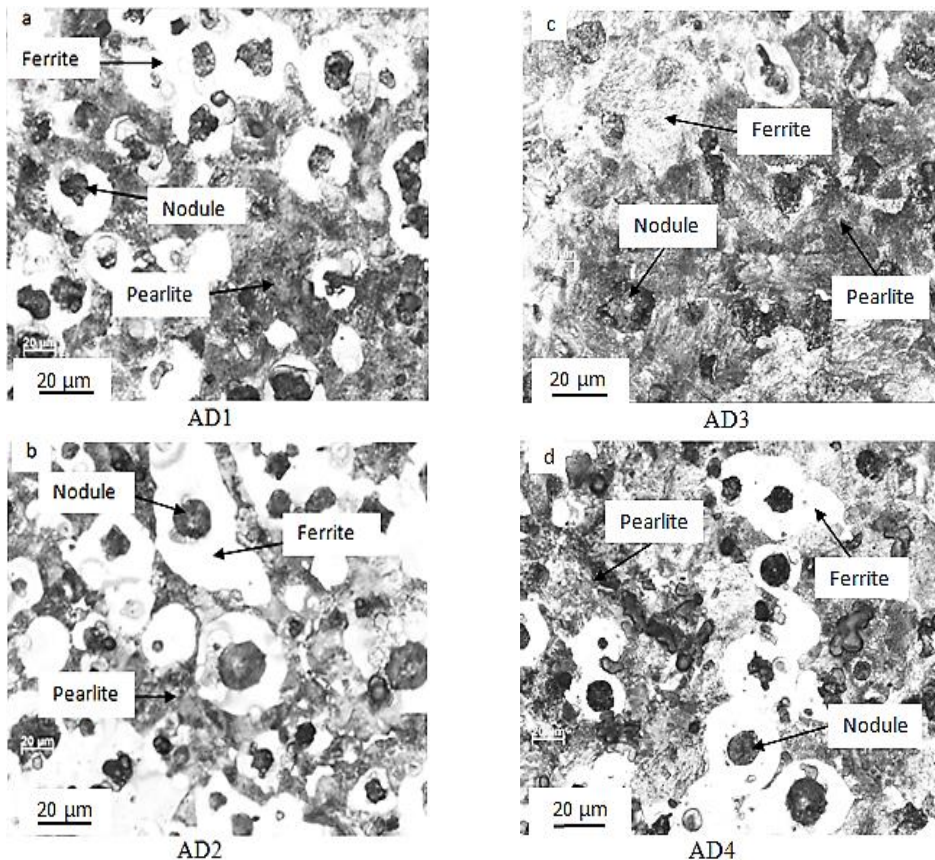
RESULTS AND DISCUSSION
Microstructure Characterization

The microstructures of the cast irons produced are presented in **Figure 1**. It is observed that **Figures 1(a) – 1(e)** contain nodular/spheroidal graphite morphology, which indicates that the structures are that of ductile irons. It is noted that the matrix structure of the ductile irons consists of pearlite and ferrite phases with proportions as presented in **Table 3**. The nodular graphite structures are observed to be circumscribed by ferrite in their immediate vicinities. This is in accordance with microstructure study by many authors [22-24]. However, it is more pronounced for the compositions AD1,

AD2 and AD4, which contain Mo-Ni-Cu, Mo-Ni, and Mo-Ni-Cr, respectively as micro-alloying elements. AD3 which contains Cu-Cr did not have as much ferrite surrounding the nodular graphite as in the other micro-alloyed ductile iron compositions. It is also confirmed from **Table 3** that it has the least volume fraction of ferrite for all the cast iron compositions produced. Figures 1(f) and 1(g) on the other hand, show flaky graphite structure, which is characteristic of grey irons. It is noted that the two compositions, AG1 and AG2, both contain micro alloying elements – Mo-Cr-Cu and Ni-Cr-Cu, respectively. The quantified microstructural parameters for the cast irons produced are presented in **Table 3**.

Table 3 Results of Microstructure Characterization of all the Samples (Omole et al. [11]).

Sample	Volume fraction of Pearlite	Volume fraction of Ferrite	Volume fraction of Nodule/ Pearlite	Nodularity %	Nodules count (per mm ²)
AD1	49.38 % ±2.55	38.93 % ±2.35	11.14 % ±1.82	91	110
AD2	49.70 % ±2.82	40.11 % ±2.64	10.98 % ±1.68	90	115
AD3	56.06 % ±1.85	29.83 % ±2.43	14.51 % ±2.08	88	105
AD4	56.59 % ±2.32	32.68 % ±2.42	11.31 % ±1.95	92	120
D5	30.63 % ±2.12	59.37 % ±2.71	10.27 % ±2.10	88	107
AG1	37.37 % ± 2.26	39.86 % ±2.25	22.73 % ±2.20	-	-
AG2	33.12 % ± 2.22	51.82 % ±2.18	15.50 % ±2.16	-	-



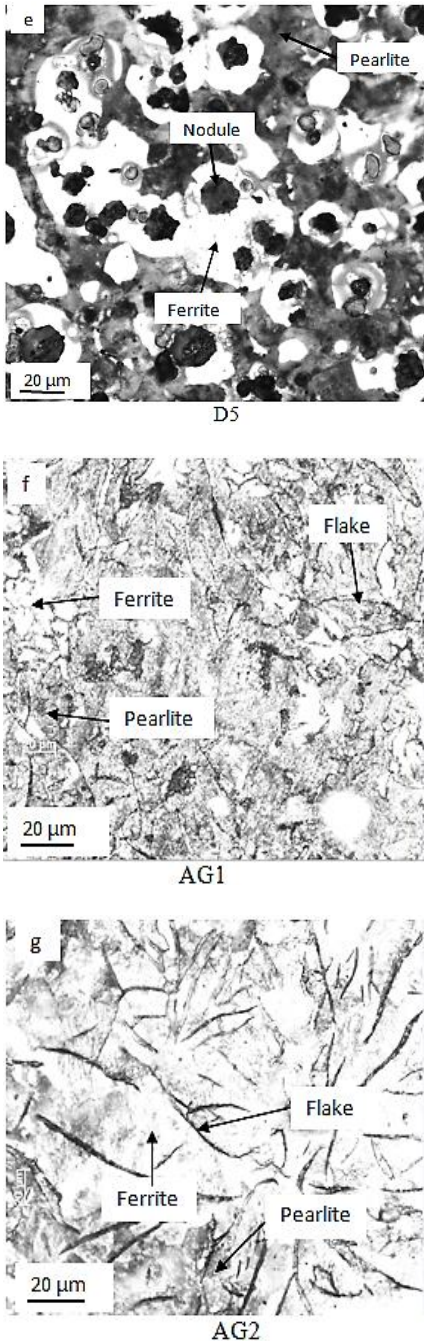


Fig. 1 Microstructures of Ductile and Grey Cast Irons Produced (a to c are the microstructures of ductile iron with nodules while f and g are the microstructures of grey iron containing flakes)

Damping Behaviour

The results of the damping tests are presented in **Figures 2 – 4**. It is observed from **Figures 2(a) and (b)** that the storage modulus, which serves as a measure of the capacity of a material to absorb/store vibration energy is marginally influenced by the test frequencies (1 and 5 Hz) utilized in the study. From **Figure 2(a)**, it is noted that the ductile iron composition designated AD2 (which contains Mo-Ni), had the highest storage modulus values (120868.51 MPa), compared to the other ductile and grey irons investigated. Generally, it is noted that the storage modulus of the micro alloyed ductile irons (78906.39 – 120868.51 MPa) were higher than that of the micro alloyed grey irons (61118.79 – 79314.9 MPa), and the ductile iron composition without micro alloying elements, had the least storage modulus (19890.19 – 19699.15 MPa). This can be confirmed in **Table 4**.

The way of absorbing energy during damping test by cast irons is said to depend on the graphite count of the iron, graphite surface areas and the contact interaction of ferrite phase with the graphite [16]. The additional effect of contact interaction between the ferrite and graphite phases, which is more pronounced in the micro-alloyed ductile irons, may be linked to the higher storage modulus exhibited by the micro-alloyed ductile irons compared with the micro-alloyed grey irons. It is also noted that with the exception of the ductile irons designated AD1 and AD4, there was basically slight reduction in storage modulus with increase in temperature within the range of 40 – 190 °C used in the study.

Alaneme and Fajemisin [25] reported that decrease in storage modulus is associated with increase in temperature, because of the decrease in dynamic stiffness of the material with temperature, which arises on account of the weakening of inter-atomic bonds in the material. The implication of the higher storage modulus of the micro alloyed ductile irons is that they possess higher energy absorption capacity compared to the other cast iron grades produced. Virtually the same trend and arguments subsists for the storage modulus values assessed at both test frequencies of 1 and 5 Hz.

The loss moduli of the ductile and grey irons produced are presented in **Figure 3**. It is observed that why apparently the loss modulus appears to follow the same trend at both 1 and 5 Hz test frequencies, the loss modulus values in most cases, are slightly higher at test frequencies of 1 Hz compared to 5 Hz, as can be confirmed from **Table 5**. The effect of cast iron composition and test temperature was however, more distinct and consistent than that of test frequency. It is observed from **Figure 3** that for both test frequencies, the micro alloyed ductile irons with the exception of AD2 had higher loss modulus values which decreased with intermittent high peaks at temperatures between 40 to 190 °C than the other cast iron compositions produced. Ibrahim et al. [16] reported that increase in energy dissipation is enhanced in cast irons with greater graphite count and higher amount of ferrite surrounding the graphite nodules. That is, the ferrite surrounding the graphite serve as additional vent for energy dissipation due to the easier plastic flow that occurs in the interface between the graphite and ferrite phases [2]. In the grey irons, the energy dissipation is ideally linked squarely to the internal friction mechanism which occurs in the graphite precipitate [14, 15]. But in the ductile irons, the ferrite surrounding the graphite contributes to the greater energy dissipation observed. The least loss modulus and storage modulus was observed in the ductile iron composition without micro-alloying addition.

The decrease in loss modulus with temperature may be as a result of reduction in internal friction of the material as the kinetic energy increases with increase in temperature. The

implication is that there is slight reduction in energy dissipation capacity of the irons with increase in temperature. The damping capacities of the cast irons produced are presented in **Figure 4**. It is observed that the damping capacity variation pattern was slightly different at the test frequencies of 1 and 5 Hz. It is observed that at 30 °C, the damping capacities of the micro alloyed ductile irons AD3, AD1 and AD4 are higher than that of other cast irons investigated. The damping capacities are observed to drop sharply from ~ 0.07 – 0.08 at 30 °C to ~ 0.06 at 50 °C; after which fairly more stable values with intermittent high and low peaks were obtained for these ductile iron compositions. The ductile iron composition without micro alloying elements (D5), exhibited the reverse trend as its damping capacity values increased from 0.057 at 30 °C to approximately 0.09 at 110 °C, which was the temperature at which the sample failed. Despite the higher damping capacity values above that of samples AD3, AD1 and AD4, the fact that it failed at a relatively lower temperature of 110 °C compared to the other cast irons tested to temperature of 190 °C, raises concerns on its suitability compared to the other cast irons produced. The ductile iron composition AD2 is observed to have the lowest damping capacity, which can be linked to its high energy absorption capacity and relatively low energy dissipation characteristics. It is also noted that the micro-alloyed grey irons had damping capacity values lower than that of the other micro alloyed ductile irons – AD3, AD1, AD4. The generally higher damping capacity of the micro-alloyed ductile irons can be attributed to contributions of the graphite nodules and the ferritic matrix surrounding the graphite [16], as is observed in **Figure 1**. The ferrite phase circumjacent to the spherical graphite ensures that plastic flow occurs more readily in the interface between the graphite and ferrite phases, thereby resulting in higher damping capacity. Thus, the higher the number of graphite nodules and nodules surrounded by ferrite, the higher the damping capacity due to the higher (energy absorption/dissipation centres) contact surface between graphite and ferrite, which help attenuate vibration effects and thus resulting in higher damping capacity in the ductile irons. It is also worth remarking that the effect of the test frequency was more consistent at near room temperature, where it is observed that the damping capacity values for AD3, AD1 and AD4, are lower at test frequency of 5 Hz than that observed at 1 Hz (as shown in **Table 6**).

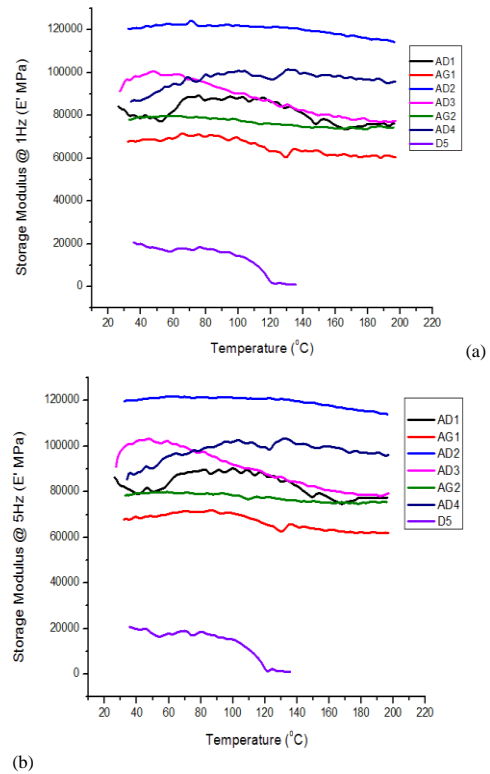


Fig. 2 Storage Modulus as a function of Temperature at (a) 1 and (b) 5 Hz Frequencies

Table 4 Storage Modulus of all the Specimens @ 40 °C and 190 °C for Test Frequencies of 1 and 5 Hz

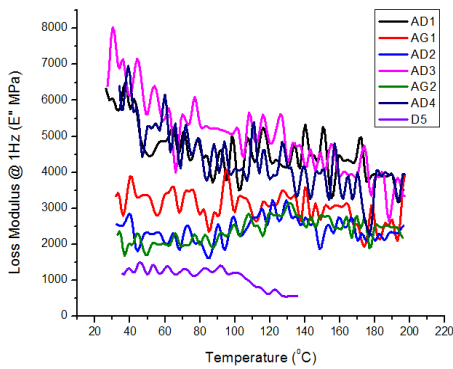
Sample	Storage Modulus (MPa) @ 40 °C		Storage Modulus (MPa) @ 190°C	
	1 Hz	5 Hz	1 Hz	5 Hz
AD1	78906.39	79165.72	76184.99	77360.41
AD2	120868.51	120245.91	115283.00	114702.71
AD3	98523.26	102349.12	77429.42	78493.48
AD4	87073.29	88296.05	95879.31	97159.99
D5	19890.19	19699.15	-	-
AG1	68490.37	68965.09	61118.79	62006.61
AG2	79272.43	79314.91	74634.42	75452.19

Table 5 Loss Modulus of all the Specimens @ 40 °C and 190 °C for Test Frequencies of 1 and 5 Hz

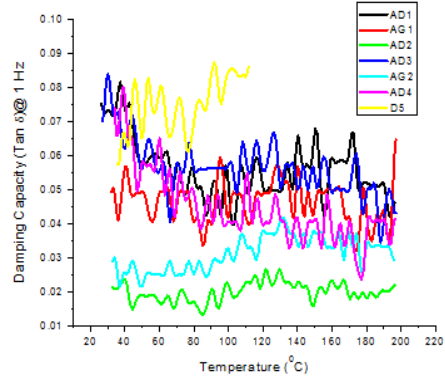
Sample	Loss Modulus (MPa) @ 40 °C		Loss Modulus (MPa) @ 190 °C	
	1 Hz	5 Hz	1 Hz	5 Hz
AD1	5757.99	5375.53	3909.57	3261.29
AD2	2833.05	2727.13	2332.38	2460.96
AD3	6124.51	6016.62	3197.31	3523.58
AD4	6715.14	5351.41	3949.63	3518.53
D5	1338.41	1272.11	-	-
AG1	3889.74	3023.77	2690.81	2258.51
AG2	2026.64	1841.51	2471.03	2063.11

Table 6 Damping Capacity of all the Specimens @ 40 °C and 190 °C for Test Frequencies of 1 and 5 Hz

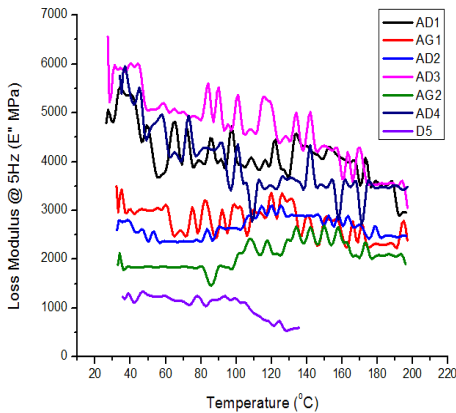
Sample	Damping Capacity ($\tan \delta$) @ 40°C		Damping Capacity ($\tan \delta$) @ 190°C	
	1 Hz	5 Hz	1 Hz	5 Hz
AD1	0.07298	0.06790	0.05131	0.04216
AD2	0.02343	0.02268	0.02023	0.02146
AD3	0.06217	0.05878	0.04128	0.04489
AD4	0.07714	0.06062	0.04120	0.03621
D5	0.06477	0.06007	-	-
AG1	0.05678	0.04384	0.04402	0.03643
AG2	0.02557	0.02322	0.03311	0.02734



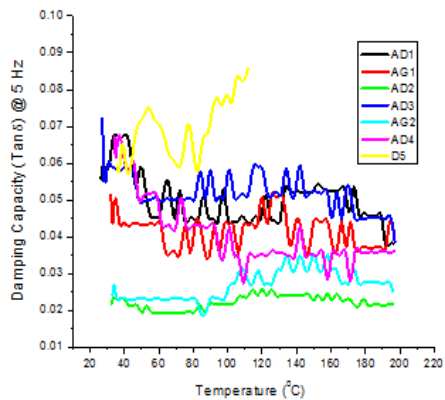
(a)



(a)



(b)



(b)

Fig. 3 Loss Modulus as a function of Temperature at (a) 1and (b) 5 Hz Frequencies.

Fig. 4 Damping Capacity ($\tan \delta$) as a function of Temperature at (a) 1and (b) 5 Hz Frequencies.

CONCLUSIONS

In this study, the damping characteristics of ductile and grey cast irons, micro alloyed with Mo, Ni, Cu and Cr, investigated using dynamic mechanical thermal analysis, were reported. The results indicated that:

The Microstructures of the ductile irons contain pearlite, ferrite and graphite nodules with nodules count in various proportions. The presence of ferrite phase surrounding the nodular graphite with the nodule count, accounted for the high damping capacity obtained.

Ductile iron without micro alloying elements had the least storage modulus (19890.19 – 19699.15 MPa), while the micro alloyed ductile irons had higher storage modulus (78906.39MPa – 120868.51 MPa) than the micro alloyed grey cast iron (61118.79 – 79314.9 MPa). So, the energy absorption was noticed to be dependent on the graphite count and interaction of ferrite phase with the graphite among others.

The loss modulus of all the samples was distinctly affected by the composition and test temperature than the test frequency. However, for both test frequencies, most of the micro alloyed ductile irons basically had higher loss modulus values than the grey cast iron.

Damping capacity of sample D5 (without micro alloying elements) increased progressively from 0.06007-0.06477 at room temperature to ~ 0.085 at about 110 °C and failed, while samples AD1 AD3 and AD4 damping capacity was higher at room temperature but dropped at 50 °C and after which stable values was observed even at high temperatures. Therefore, samples AD1, AD3 and AD4 displayed the compositions most suitable for mechanical damping.

ACKNOWLEDGEMENTS

The authors wish to thank the Head, School of Mining, Metallurgy and Chemical Engineering, and Centre for Nano Engineering and Tribo-corrosion, University of Johannesburg, Johannesburg South Africa, Prof. P. A. Olubambi, who assisted in the provision of facilities needed for the research.

REFERENCES

1. J. L. Hernandez-Rivera, R. E. Compos Cambranis, A. De la Garza: *Materials Design*, 32, 2011, 4756–4762. <https://doi.org/10.1016/j.matdes.2011.06.030>.
2. C-Y. Kang, J-H. Sung, G-H. Kim, B-S. Kim, I-S. Kim: *Materials Transaction*, 50(6), 2009, 1390–1395. <https://doi.org/10.2320/matertrans.MRA2008427>.
3. F. Iacoviello, D. Iacoviello, V. D. Cocco, A. D. Santis, L. D. Agostino: *Procedia structural integrity*, 3, 2017, 283–290. <https://doi.org/10.1016/j.prostr.2017.04.042>.
4. C. Fragassa: *Journal of Mechanical Engineering Science*, 231(1), 2017, 18–30. <https://doi.org/10.1177/0954406216639996>.
5. M. M. Rashidi, M. H. Idris: *Materials Science and Engineering A*, 597, 2014, 395–407. <https://dx.doi.org/10.1016/j.msea.2013.12.070>.
6. J. Laine, K. Jalava, J. Vaara, K. Soivio, T. Frondelius, J. Orkas: *International journal of Metal casting*, 2020. <https://doi.org/10.1007/s40962-020-00473-8>.
7. G. Lannitti, A. Ruggiero, N. Bonora, S. Masaggia, F. Veneri: *Theoretical and Applied Fracture Mechanics*, 92, 2017, 351-359. <https://dx.doi.org/10.1016/j.tafmec.2017.05.007>.
8. L. Rao, W. Tao, S. Wang, M. Geng, G. Cheng: *Indian Journal of Engineering and Materials Science*, 21, 2014, 573-579.
9. K. J. Mohammed: *Unified Journal of Engineering and Manufacturing Technology*, 1(1), 2016, 001-006.
10. S. O. Omole, A. Oyetunji, K. K. Alaneme, P. A. Olubambi: *Tribology in industry*, 40(4), 2018, 584–593. <https://doi.org/10.24874/ti.2018.40.04.07.2018>.
11. S. O. Omole, A. Oyetunji, K. K. Alaneme, P. A. Olubambi: *Journal of King Saud University-Engineering Sciences*, 32, 2020, 205-210. <https://doi.org/10.1016/j.jksues.2018.11.00>.
12. M. Ramadan, N. Fathy: *Journal of Minerals and Materials Characterization and Engineering 2*, 2014, 26–31. <https://dx.doi.org/10.4236/jmmce.2014.21005>.
13. P. Kovacicikova, J. Vavro, J. Vavro Jr, A. Dubec: *Manufacturing Technology*, 18(1), 2018, 57–59. <https://doi.org/10.21062/ujep/53.2018/a/1213-2489/MT/18/1/57>.
14. P. Millet, R. Schaller, W. Benoit: *Journal de Physique Colloques*, 46(C10), 1985, C405-C408.
15. T. Murakami, T. Inoue, H. Shimura, M. Nakano, S. Sasaki: *Materials Science and Engineering A*, 432, 2006, 113–119. <https://doi.org/10.1016/j.msea.2006.06.090>.
16. M. M. Ibrahim, M. M. Mourad, A. A. Nofal, A. I. Z. Farahat: *International Journal of Cast Metals Research*, 30(2), 2017, 61-69. <https://doi.org/10.1080/13640461.2016.1239895>.
17. J. Cui, L. Chen: *Journal of Materials Science and Technology*, 33(12), 2017, 1549-1554. <https://dx.doi.org/10.1016/j.jmst.2017.08.03>.
18. T. Sun, R-B. Song, X. Wang, P. Deng, C-J Wu: *Materials Science and Engineering A*, 626, 2015, 375-381. <https://dx.doi.org/10.1016/j.msea.2014.12.078>.
19. I. Pereira, G. Alonso, V. Anjos, L. F. Malheiros, R. Suarez: *International journal of metal casting*, 14, 2020, 802–808. <https://doi.org/10.1007/s40962-020-00426-1>.
20. ASTM E756-05: Standard test method for measuring vibration damping properties of materials. *ASTM standard 2017* www.astm.org.
21. D. Silva-Prasad, C. Shoba: *Engineering Science and Technology - International Journal*, 18, 2015, 674–679. <https://doi.org/10.1016/j.jestech.2015.05.001>.
22. H. Ananda, S. Sathyashandra, V. S. Ramakrishna: *Journal of Mechanical Engineering and Sciences*, 13(1), 2019, 4356-4367. <https://doi.org/10.15282/jmes.13.1.2019.01.0371>.
23. N. S. Tiedje: *Materials Science and Technology*, 26(5), 2010, 505-514. <https://doi.org/10.1179/026708310X12668415533649>.
24. C. Fragassa, N. Radovic, A. Pavlovic, G. Minak: *Tribology in Industry*, 38(1), 2016, 45-56.
25. K. K. Alaneme, A. V. Fajemisin: *Engineering Science and Technology, an International Journal*, 21, 2018, 798-805. <https://doi.org/10.1016/j.jestech.2018.05.007>.